The Interface between a Protein Crystal and an Aqueous Solution and Its Effects on Nucleation and Crystal Growth

C. Haas and J. Drenth*

Laboratory of Biophysical Chemistry, University of Groningen, Nijenborgh 4, 9747 AG, Groningen, The Netherlands

Received: September 10, 1999; In Final Form: November 3, 1999

In this paper we report calculations of the concentration profile and the Gibbs free energy of the interface between a protein crystal and an aqueous solution. The calculations are based on a simple, realistic expression for the Gibbs free energy of the solution, which reproduces characteristic features of the protein−water phase diagram, such as the presence of a metastable liquid−liquid immiscibility region. An equation is derived which expresses the coefficient for the contribution of concentration gradients to the Gibbs free energy of the solution in terms of the interaction potential between the protein molecules. Calculations are presented which show that the presence of a metastable liquid−liquid immiscibility region in the phase diagram has a profound effect on the properties of the interface between a crystal and the solution. Near and below the critical temperature for metastable liquid−liquid phase separation the protein crystal is covered by a thin liquid film with a high protein concentration. This surface film causes a substantial lowering of the surface energy of the crystal. The effects of this film on the kinetic processes associated with the nucleation and the further growth of protein crystals are discussed.

1. Introduction

The difficulties encountered in the growing of good crystals for protein crystal structure determination by X-ray diffraction have stimulated research in the mechanism of the nucleation and growth of protein crystals. However, crystallization is a very complex phenomenon, involving the phase diagram of the protein−solvent system, the interface between the crystal and the liquid, the transport of molecules in the liquid phase, and the kinetics of nucleation and growth. Many aspects of crystal growth are not well understood at present and deserve further study before optimal crystallization conditions can be predicted.

Experimental[1−8] and theoretical[9−11] studies have shown that for sufficiently strong attractive interactions between the protein molecules, the protein−water phase diagram shows at room temperature a metastable region of liquid−liquid immiscibility. A metastable immiscibility region is present in the phase diagram only if the interactions between the protein molecules are short range and/or highly anisotropic.[10−16] There is experimental evidence that the presence of a metastable region of liquid−liquid immiscibility is connected with the conditions for growing good protein crystals.[10,11,17,18] It has been suggested that in the presence of a metastable liquid−liquid immiscibility region the nucleation of crystals proceeds via a two-step mechanism, involving as a first step the formation of a small metastable liquid droplet with a high protein concentration; the nucleation of the crystal would then take place inside this droplet.[10,11,19−22]

Evans et al.[23−25] have shown that the concentration profile of the interface between a crystal and an aqueous solution is strongly influenced by the presence of a metastable region of liquid−liquid immiscibility. These authors found that in this case the crystal is covered by a film of a solution with a high concentration. However, they could not give a quantitative estimate of the thickness of the film because no information was available for the parameter κ which is needed to calculate the width.

According to classical nucleation theory[26] an important parameter which determines the activation energy for nucleation and the size of the critical nucleus is the energy of the interface between the crystal and the supersaturated solution. The presence of the liquid film on the surface of the crystal lowers the surface energy of the interface between the crystal and the solution. The interface between crystal and solution also plays an important role in the kinetic processes associated with crystal growth.[27]

In this paper we present calculations of the concentration profile and the surface energy based on a simple expression for the Gibbs free energy of an aqueous protein solution. We derive an expression for the contribution of concentration gradients to the Gibbs free energy of the solution in terms of the interaction potential between the protein molecules. With these ingredients it is possible to calculate quantitatively the concentration profile and the energy of the interface between a protein crystal and an aqueous solution, or between two coexisting liquid phases with different protein concentrations. The implications of these results for crystal nucleation and crystal growth are discussed.

2. Protein−Water Phase Diagram

The phase diagram of a system of large particles dissolved in a solvent of small molecules has been studied theoretically by many authors. For colloidal systems numerical calculations on the basis of an effective isotropic attractive interaction potential between the large particles have shown that the phase diagram will generally have a liquid−liquid immiscibility region. Depending on the range of the interactions this region can be stable or metastable.[10,28−33] These theoretical considerations have

* To whom correspondence should be addressed. E-mail: J.Drenth@CHEM. RUG.NL

10.1021/jp993210a CCC: $19.00
Published on Web 12/16/1999

been applied also to solutions of proteins in aqueous solvents.[9,14−16,28,34,35] However, it was shown recently that although the interactions between colloidal particles can be described with an isotropic interaction potential, this is not true for protein molecules.[12,13,36,37] The interaction between protein molecules is highly anisotropic; it depends on the mutual orientation of the two interacting molecules. This anisotropy has a profound influence on the phase diagram, as it reduces the average interaction between the molecules in the liquid phase as compared with the interactions in the crystal.

In this paper we use relatively simple expressions for the Gibbs free energies of protein crystals and protein aqueous solutions.[6,38] These expressions describe in a satisfactory way the essential features of the protein−water diagram, such as the presence of a stable or metastable liquid−liquid two-phase region.[11]

For the crystalline state we write

$$G_c = (1/\Omega)\phi_c g_c \tag{1}$$

For the solution we write

$$G_l = (1/\Omega)\left[(\phi^2/\phi_c)g_l + kT\phi\ln\phi - kT\phi\ln m - kT\left\{\frac{\phi - 6\phi^2 + 4\phi^3}{(1-\phi)^2}\right\}\right] \tag{2}$$

where G_l is the Gibbs free energy per unit volume of a solution with a protein volume fraction ϕ, G_c is that of the crystalline phase with a protein volume fraction ϕ_c; for most proteins the value of ϕ_c is about 0.5. The parameters g_c and g_l describe the interactions between protein molecules in the solid and in the solution, respectively. The volume of a protein molecule is Ω and $m = \Omega/\omega$, where ω is the molar volume of water divided by Avogadro's number. The first term in eq 2 describes the effective interaction between the protein molecules in the solution, including the contributions due to changes in solvent−solvent or protein−solvent interactions. In g_l the effect of the anisotropy of the interactions is taken into account.[12] The last three terms in eq 2 give the expression for the entropy of mixing as proposed by Carnahan and Starling.[39]

From eqs 1 and 2 one can calculate the phase diagram.[11] It is found that for negative values of g_l, i.e., for an attractive interaction between the protein molecules, the phase diagram has a region of liquid−liquid phase separation below a critical temperature T_0. Below T_0 two liquid phases with the binodal concentrations ϕ_α and ϕ_β coexist. For relatively small values of g_l/g_c the two-phase region is metastable (Figure 1); for relatively large g_l/g_c the phase diagram has a stable two-phase region at temperatures above the triple point temperature T_t (Figure 2) . At the triple point two liquid phases with compositions $\phi_s = \phi_\alpha$, ϕ_β and a solid phase with composition ϕ_c are in equilibrium.

The solubility of the crystal ϕ_s can be obtained from eqs 1 and 2; if the solubility is small ($\phi_s \ll 1$), it is given approximately by

$$\phi_s = m\exp(g_c/kT) \tag{3}$$

For convenience we introduce an interaction parameter θ with the dimension of a temperature

$$\theta \equiv -\frac{g_l}{10.601 \times k\phi_c} \tag{4}$$

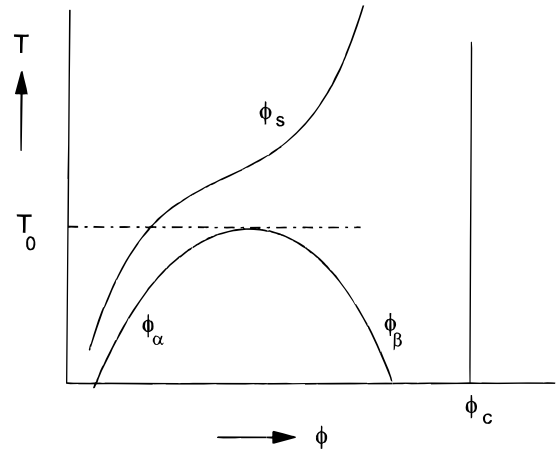

Figure 1. Phase diagram with a metastable liquid−liquid immiscibility region (small value of g_l/g_c). The coexisting liquid phases have compositions ϕ_α and ϕ_β. The liquid phase ϕ_s is in equilibrium with the solid phase ϕ_c. T_0 is the critical temperature for liquid−liquid phase separation.

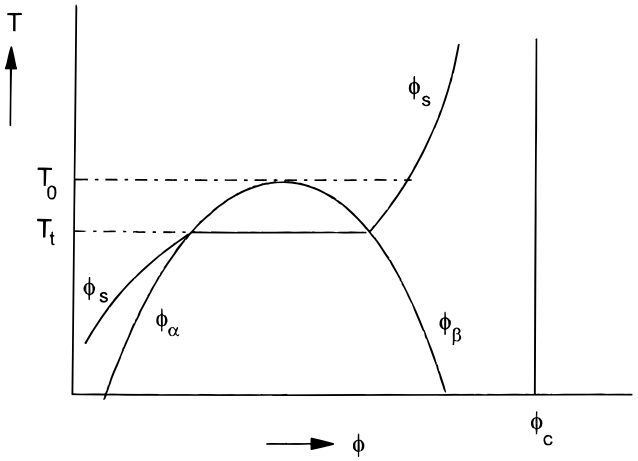

Figure 2. Phase diagram with a stable liquid−liquid immiscibility region (large value of g_l/g_c). The coexisting liquid phases have compositions ϕ_α and ϕ_β. The liquid phase ϕ_s is in equilibrium with the solid phase ϕ_c. T_0 is the critical temperature for liquid−liquid phase separation; T_t is the triple point temperature.

where θ is defined in such a way that at the critical temperature, T_0, $\theta = T_0$. Generally g_l, g_c, and θ depend on the temperature, and the critical temperature T_0 is given by

$$T_0 = \theta(T_0) = -\frac{g_l(T_0)}{10.601 \times k\phi_c} \tag{5}$$

where θ is proportional to g_l, the parameter for interactions between the protein molecules in the solution, and is therefore also related to the second virial coefficient B[11]

$$B = (1/M\rho)[4 - 10.601(\theta/T)] \tag{6}$$

In this equation M is the molecular weight and ρ is the density of the protein. Thus the values of the interaction parameters g_l and g_c can be obtained from experimental data of the second virial coefficient B (with eqs 5 and 6) and the solubility ϕ_s (with eq 3), respectively.

At the critical temperature T_0 for liquid−liquid phase separation, $T/\theta = 1$ and the second virial coefficient B is given by $B = -6.6/M\rho$; this corresponds to $B'/\Omega = -6.6$, where $B' = B(M\rho\Omega)$ is the second virial coefficient in units Ω.

3. Aggregates in Concentrated Protein Solutions

If metastable liquid−liquid phase separation is an intermediate step in protein crystallization, the crystals will begin to grow in a highly concentrated liquid phase with concentration ϕ_β. It is expected that in such a solution with a high protein concentration, the equilibrium concentration of aggregates or oligomers (dimers, trimers, tetramers, etc.) can be quite large. We show in this section that it is possible to estimate the average coordination number of protein molecules in concentrated solutions from experimental data on dilute solutions, i.e., from values of the second virial coefficient B and the solubility ϕ_s.

A study of the relation between the solubility and the second virial coefficient showed that the interaction between lysozyme molecules is short range and highly anisotropic.[12] This implies that the interaction between protein molecules gives an appreciable contribution to the Gibbs free energy only if the molecules are at a short distance from one another and if they have the proper orientation. For the solid the bonding energy per molecule is given by $G_c/N_c = g_c = -(1/2)z_c\epsilon$, where $N_c = (\phi_c/\Omega)$ is the number of protein molecules per unit volume, z_c is the coordination number of protein molecules in the solid phase, and ϵ is the average binding energy between neighboring protein molecules. For the solution the average binding energy per protein molecule is given by the first term in eq 2 divided by the number of protein molecules per unit volume in the solution. Thus the average binding energy per molecule in the solution is $(1/\Omega)(\phi^2/\phi_c)g_l/N_l = (\phi/\phi_c)g_l = -(1/2)z_l\epsilon$ where $N_l = (\phi/\Omega)$ is the number of protein molecules per unit volume in the solution and z_l is the average coordination number, i.e., the average number of protein molecules at a short distance from a given protein molecule, which have the proper orientation to form bonds of average strength ϵ. From these equations we find

$$z_l = z_c(\phi/\phi_c)(g_l/g_c) \tag{7}$$

For the conditions normally used in protein crystallization, $T \approx T_0$ or $T < T_0$, $g_l/g_c \approx 0.5$ (see ref 11), and $z_c = 4-6$, one expects values for z_l between 1.2 and 1.8 for a solution with protein concentration $\phi_\beta = 0.3$. These values can be compared with the coordination numbers for given aggregates. For dimers $z = 1$, for trimers $z = 1.33$, for tetramers $z = 1.5$, and for an infinitely long chain $z = 2$. One expects higher values of z for more compact aggregates; for an aggregate of eight molecules, arranged at the corners of a cube, the coordination number $z = 3$. The calculated values of z_l indicate that in a protein solution with a high concentration most molecules are part of aggregates. These could be small aggregates (tetramers, etc.), but it is also possible that a large fraction of the molecules are part of extended, open structures (fractals). The latter case could lead to a gel-like constitution of the high concentration droplets.

The bonds between the molecules in these aggregates are not permanent; because the binding energy between two molecules ϵ is only a few kT, there is a continuous thermal rearrangement, with the formation and dissociation of aggregates.

4. Concentration Profile and Gibbs Free Energy of the Interface

In this section we consider the interface between two coexisting phases with different concentrations. The concentration near the interface does not change abruptly from the equilibrium concentration in one phase to the equilibrium concentration in the other phase, but the change is continuous. The concentration profile between two liquid phases has been discussed by Cahn and Hilliard,[40] the concentration profile between a solid and a liquid phase by Cahn[41] and by de Gennes.[42] We summarize here the theory and apply it to calculate the concentration profile of the interface between two protein solutions with different concentrations (section 6) and of the interface between a protein crystal and a saturated solution (section 7).

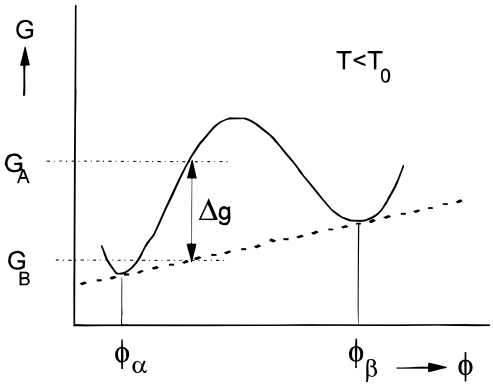

Figure 3. Gibbs free energy G_l of the liquid phase as a function of the protein volume fraction ϕ. The coexisting phases for liquid−liquid phase separation have compositions ϕ_α and ϕ_β. The quantity Δg in eq 9 is given by $\Delta g = G_A - G_B$, where G_A is the Gibbs free energy per unit volume of a single phase with concentration ϕ and G_B is that of an equilibrium mixture of two phases with concentrations ϕ_α and ϕ_β with the same overall composition ϕ.

The total Gibbs free energy of a volume V of a system in which the concentration is not a constant but depends on the position can be written as

$$G_{total} = \int_V \left[G_l(\phi) + (\kappa/\Omega)\left(\frac{d\phi}{dx}\right)^2\right] dv \tag{8}$$

where $G_l(\phi)$ is the Gibbs free energy per unit volume of a liquid phase with volume fraction ϕ of the solute. The second term gives the contribution due to the concentration gradient; x is the position in the system. The value of the parameter κ is determined by the interactions between the protein molecules.

The concentration profile of the interface between two coexisting phases will adjust itself in such a way that the total Gibbs free energy of the system is a minimum. Applying this condition to eq 8 results in a differential equation from which the concentration profile can be calculated[40]

$$\left(\frac{dx}{d\phi}\right) = \left(\frac{\kappa}{\Omega\Delta g}\right)^{0.5} \tag{9}$$

In this equation Δg is the difference in Gibbs free energy per unit volume between a single phase with concentration ϕ and an equilibrium mixture of two coexisting liquid phases ϕ_α and ϕ_β with average concentration ϕ (see Figure 3). The concentration profile can be calculated by integrating eq 9. It is found that the concentration in the interface changes gradually from the value ϕ_α in one phase to the value ϕ_β in the other phase. The Gibbs free energy of the interface per unit surface area is given by[40]

$$\sigma = \int_{-\infty}^{+\infty} \left[\Delta g + (\kappa/\Omega)\left(\frac{d\phi}{dx}\right)^2\right] dx \tag{10}$$

Using eq 9 this can also be written as

$$\sigma = \int_{\phi_\alpha}^{\phi_\beta} 2\left(\frac{\kappa\Delta g}{\Omega}\right)^{0.5} d\phi \tag{11}$$

Thus, with eqs 9 and 11 the concentration profile $\phi(x)$ and the

interface energy σ can be calculated provided the Gibbs free energy curve $G_l(\phi)$ and the parameter κ are known.

5. Calculation of the Parameter κ from the Interaction Potential

To calculate the width of the transition layer between two phases it is necessary to know the value of the parameter κ of the gradient term in the free energy. In this section we derive a relation between κ and the interaction potential between protein molecules in the solution.

The stability of solid and liquid phases in the protein−water phase diagram is a consequence of the interactions between the protein molecules. We first assume that the interactions can be represented by an isotropic interaction potential $U(r)$ which depends only on the distance between the centers of the two interacting protein molecules. The parameter g_c for the interactions in the crystal is given by

$$g_c = \frac{1}{2}\sum_{i=1}^{z} U(r_i) \tag{12}$$

where r_i is the distance to a neighboring molecule i and the sum is over all z near neighbors. The contribution of interactions between pairs of molecules to the Gibbs free energy of a solution with a volume V containing N molecules is given by[43]

$$\Delta G_{\text{total}} = -\frac{kTN^2}{2V^2}\int\int [e^{-U_{12}/kT} - 1]\mathrm{d}v(r_1)\mathrm{d}v(r_2) \tag{13}$$

where U_{12} is the interaction between molecules at positions r_1 and r_2. The interaction is assumed to depend only on the distance r between the two molecules. The number of molecules N is related to the volume fraction by $\phi = N\Omega/V$. In eq 13 it is assumed that the concentration of the molecules is constant. For a nonuniform system in which the concentration ϕ depends on the position in the system, eq 13 can be generalized as

$$\Delta G_{\text{total}} = -\frac{kT}{2\Omega^2}\int\int \phi(\mathrm{r}_1)\phi(r_2)[e^{-U_{12}/kT} - 1]\mathrm{d}v(r_1)\mathrm{d}v(r_2) \tag{14}$$

Defining $\mathbf{r} = \mathbf{r}_2 - \mathbf{r}_1$ and changing the integration from $\mathrm{d}v(r_1)$-$\mathrm{d}v(r_2)$ to $\mathrm{d}v(r_1)\mathrm{d}v(r)$ we obtain

$$\Delta G_{\text{total}} = -\frac{kT}{2\Omega^2}\int\int \phi(r_1)\phi(r_1 + r)[e^{-U(r)/kT} - 1]\mathrm{d}v(r_1)\mathrm{d}v(r) \tag{15}$$

We assume that the concentration changes only along the x direction. For a short-range potential there are only contributions to ΔG_{total} from small values of the distance between the molecules; for large values of r the term $[e^{-U(r)/kT} - 1]$ is small. Thus for a short-range potential we can use a series expansion

$$\phi(r_1 + r) = \phi(r_1) + (\mathrm{d}\phi/\mathrm{d}x)_{r_1}x + \frac{1}{2}(\mathrm{d}^2\phi/\mathrm{d}x^2)_{r_1}x^2 + ... \tag{16}$$

Carrying out the integration over the angular part of $\mathrm{d}v(r) = r^2\mathrm{d}r\ \sin\theta\ d\theta d\varphi$, we find that the linear term in x vanishes and we obtain

$$\Delta G_{\text{total}} = -\frac{kT}{2\Omega^2}\int \phi^2(r_1)\mathrm{d}v(r_1) \times \int [e^{-U(r)/kT} - 1]\mathrm{d}v(r) - \frac{kT}{2\Omega^2}\int \phi(r_1)(\mathrm{d}^2\phi/\mathrm{d}x^2)_{r_1}\mathrm{d}v(r_1) \times \int [e^{-U(r)/kT} - 1](r^2/6)\mathrm{d}v(r) \tag{17}$$

We obtain by partial integration of the second term, apart from an irrelevant surface integral,

$$\Delta G_{\text{total}} = -\frac{kT}{2\Omega^2}\int \phi^2(r_1)\mathrm{d}v(r_1) \times \int [e^{-U(r)/kT} - 1]\mathrm{d}v(r) + \frac{kT}{2\Omega^2}\int (\mathrm{d}\phi/\mathrm{d}x)_{r_1}^2\mathrm{d}v(r_1) \times \int (r^2/6)[e^{-U(r)/kT} - 1]\mathrm{d}v(r) \tag{18}$$

This expression can be compared with eq 8 which gives the Gibbs free energy of the solution. We have to realize that eqs 8 and 2 also comprise terms not included in eq 18, namely the free energy of the ideal solution and higher order terms of the entropy of mixing proportional to ϕ^3, ϕ^4, etc. Equating the terms proportional to ϕ^2 in eqs 8 and 18 and using eq 2 for $G_l(\phi)$ we find for isotropic interactions

$$g_l = -4kT\phi_c + \frac{kT\phi_c}{2\Omega}\int_0^\infty [1 - e^{-U(r)/kT}]\mathrm{d}v(r) \tag{19}$$

$$\kappa = -\frac{kT}{2\Omega}\int_0^\infty (r^2/6)[1 - e^{-U(r)kT}]\mathrm{d}v(r) \tag{20}$$

With these equations it is possible to calculate the parameters g_l and κ from the interaction potential $U(r)$.

At this point it is useful to introduce an acceptable assumption for the interaction potential $U(r)$. For further calculations we use a simple square well potential with $U(r) = \infty$ for $r < 2a$, $U(r) = -\epsilon$ for $2a < r < 2a\lambda$, and $U(r) = 0$ for $r > 2a\lambda$. The protein molecules are assumed to be spherical, with radius a; the parameter λ is a measure of the range of the interaction. The potential has a hard core repulsion at short distances $r < 2a$ and an attractive interaction ϵ over a limited range from $r = 2a$ to $r = 2a\lambda$. The parameter g_c for this potential is given by $g_c = -1/2z_c\epsilon$; z_c is the coordination number of the protein molecules in the solid phase. Carrying out the integrations in eqs 19 and 20 gives

$$g_l = 4kT\phi_c(\lambda^3 - 1)(1 - e^{\epsilon/kT}) \tag{21}$$

$$\kappa = -\frac{8kTa^2}{5}\{1 + (\lambda^5 - 1)(1 - e^{\epsilon/kT})\} \tag{22}$$

The interaction between the protein molecules is not isotropic but highly anisotropic, and depends not only on the distance but also on the mutual orientation of the molecules. This effect reduces the integration in eqs 19 and 20 over the range $2a < r < 2a\lambda$ by a factor p.[12] For isotropic interactions $p = 1$, for anisotropic interactions $p < 1$; an analysis of the relation between the solubility and the second virial coefficient showed that for lysozyme the anisotropy is quite large, with p values of the order of 0.1 to 0.01.[12] By introducing this anisotropy eqs 21 and 22 for g_l and κ are modified to

$$g_l = 4kT\phi_c p(\lambda^3 - 1)(1 - e^{\epsilon/kT}) \tag{23}$$

$$\kappa = -\frac{8kTa^2}{5}\{1 + p(\lambda^5 - 1)(1 - e^{\epsilon/kT})\} \tag{24}$$

Using eqs 4 and 23 we can express κ in terms of the inter-

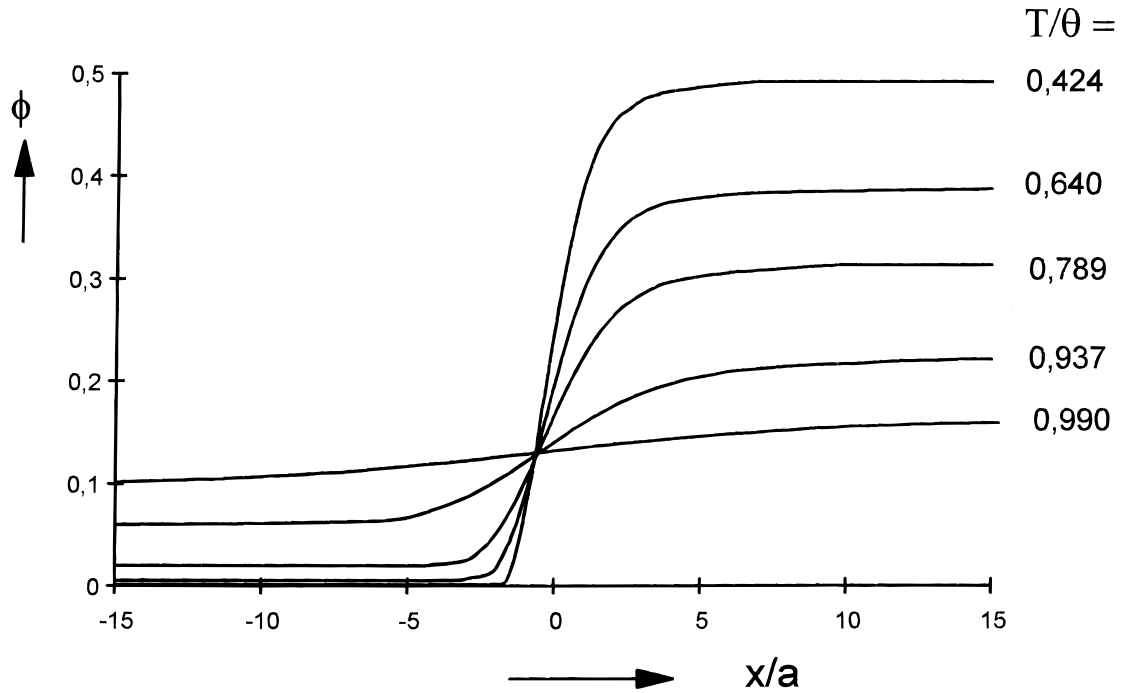

Figure 4. Calculated concentration profile for the interface between two coexisting liquid phases ϕ_α and ϕ_β for (a) $T/\theta = 0.423$; (b) $T/\theta = 0.640$; (c) $T/\theta = 0.789$; (d) $T/\theta = 0.937$; (d) $T/\theta = 0.990$.

action parameter θ

$$\kappa = \frac{8kTa^2}{5}\left[\frac{10.601}{4}\left(\frac{\lambda^5 - 1}{\lambda^3 - 1}\right)\left(\frac{\theta}{T}\right) - 1\right] \qquad (25)$$

The first term in eq 25 is due to the attractive interaction between the molecules; the negative term is an excluded volume term. We remark that the relation between κ and θ does not depend on the degree of anisotropy of the interaction between the molecules.

The range of the interactions between protein molecules $2a(\lambda - 1)$ is usually much smaller than the particle diameter, so that $(\lambda - 1) \ll 1$ and $\lambda^5 - 1 \cong 5(\lambda - 1)$ and $\lambda^3 - 1 \cong 3(\lambda - 1)$. Using these approximations we find

$$\kappa = 7.067 \times kTa^2\left(\frac{\theta}{T} - 0.226\right) \qquad (26)$$

Thus, the parameter κ can be calculated from the interaction parameter θ; the value of θ can be obtained from the second virial coefficient B with eq 6.

6. Interface between Two Liquid Phases

In this section we present results of calculations of the energy and the concentration profile of the interface between two coexisting protein solutions with volume fractions ϕ_α and ϕ_β . The calculations are based on eq 11 for the interface energy σ and on eq 9 for the concentration profile; the Gibbs free energy of the liquid phases is given by eq 2. For the calculation of the parameter κ we used eq 26.

Figure 4 shows the calculated concentration profile for different values of T/θ. We find that the thickness of the interface layer increases with increasing values of T/θ, i.e., when the concentrations ϕ_α and ϕ_β of the two layers approach each other. The interface energy σ as a function of T/θ is shown in Figure 5. The interface energy is largest for small values of T/θ, as expected; it vanishes at the critical temperature T_0, where

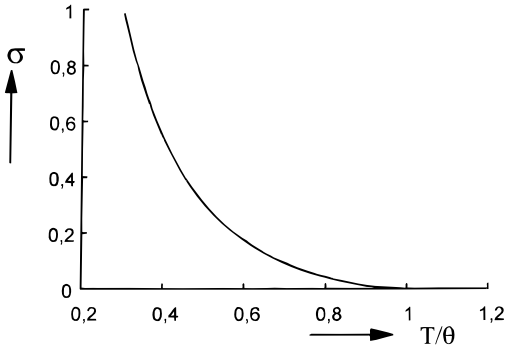

Figure 5. Energy σ (in units kT/a^2) of the interface between two coexisting liquid phases as a function of T/θ.

the composition of the two liquid phases becomes equal and $T = T_0 = \theta$.

7. Interface between a Protein Crystal and a Saturated Solution

In this section we present calculations of the concentration profile of the interface between a protein crystal and the saturated solution, and of the surface energy of the protein crystal.

The packing arrangement of the protein molecules in the surface layer of the crystal will be different from the arrangement in the bulk, as was shown for lysozyme with atomic force microscopy.[44] However, the main difference is that the molecules at the surface have a smaller coordination number. For each surface molecule there is one (or in some cases more than one) missing bond (the "bond" between two protein molecules consists of all interactions between the two molecules: hydrogen bonds, polar, van der Waals and hydrophobic interactions). For a protein crystal immersed in a pure solvent the surface energy is given by

$$\sigma_0 = \frac{1}{2}N_0\epsilon \qquad (27)$$

where N_0 is the number of protein molecules per cm^2 at the crystal surface and ϵ is the energy of the missing bond.

For a crystal in equilibrium with a solution of protein molecules, an interface layer will be formed in which the protein concentration changes gradually from the value ϕ_s in the saturated solution far away from the crystal surface to a higher value ϕ_1 at the crystal surface. The driving force for the formation of the interface layer is the possibility for molecules in the solution close to the crystal surface to form bonds with the surface molecules of the crystal, thus compensating partly for the missing bonds. The concentration profile in the solution can be calculated with eq 9. The excess of protein molecules in the interface layer (number of molecules per cm^2) is given by

$$N_A = \frac{1}{\Omega}\int_0^\infty [\phi(x) - \phi_s]\mathrm{d}x \tag{28}$$

Because of the short range of the interaction between protein molecules only molecules in a thin layer with a thickness of about $2a$ can form bonds with protein molecules of the crystal. The number N_1 of molecules in this layer is given by

$$N_1 = \frac{1}{\Omega}\int_0^{2a} \phi(x)\mathrm{d}x \tag{29}$$

Each of these N_1 molecules can form a bond, thus reducing the surface energy by an amount $N_1\epsilon$. However, this contribution is partly compensated by the reduction of the possibilities for these N_1 molecules to interact with other molecules in the solution. The reduction is by a factor $(1 - z_l/z_c)$, where z_l and z_c are the (average) coordination numbers for bonding between protein molecules in the liquid and the solid state, respectively. Therefore, the contribution to the surface energy is

$$\sigma_1 = -N_1\epsilon\left(1 - \frac{z_l}{z_c}\right) \tag{30}$$

The building up of the interface layer in the solution costs an energy

$$\sigma_2 = \int_{\phi_s}^{\phi_1} 2\left(\frac{k\Delta g}{\Omega}\right)^{0.5}\mathrm{d}\phi \tag{31}$$

The total surface energy σ is given by the sum of the three contributions

$$\sigma = \sigma_0 + \sigma_1 + \sigma_2 \tag{32}$$

The contributions σ_1 and σ_2 depend on the value of ϕ_1; ϕ_1 should be chosen in such a way that the total surface energy σ is a minimum.[41,42]

For a crystal without a surface film (i.e., with $\phi_1 = \phi_s$) the surface energy would be $\sigma_{00} = \sigma\ (\phi_1 = \phi_s)$. The net effect of the surface film, with the concentration changing gradually from ϕ_s to ϕ_1, is given by

$$\Delta\sigma = \sigma_{00} - \sigma(\phi_1) \tag{33}$$

We remark that all properties of the interface, i.e., the surface energy, the adsorbed amount of protein, and the concentration profile, can be calculated from the two parameters g_l and g_c for the interaction between protein molecules in the liquid and the solid state, respectively. The parameter g_l can be obtained from the experimental value of the second virial coefficient B (eqs 4 and 6); g_c can be calculated from the solubility (eq 3). The ratio z_l/z_c is given by $z_l/z_c = (g_l/g_c)(\phi_A/\phi_c)$, where ϕ_A is the average concentration in the layer $0 < x < 2a$.

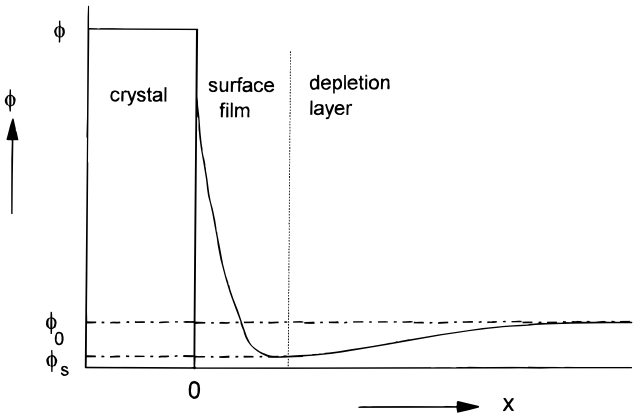

Figure 6. Protein concentration in the solution as a function of the distance from the crystal surface for a protein crystal in a supersaturated solution with concentration ϕ_0. The saturation concentration is ϕ_s, the concentration at the surface of the crystal is ϕ_1. The width of the depletion layer is much larger than the thickness of the surface film.

In the preceding part the properties of the interface were calculated for a crystal in equilibrium with the saturated solution. A growing crystal in a supersaturated solution is not in equilibrium, but if the crystal grows slowly, the surface film will be nearly in local equilibrium with the crystal and the concentration profile in this region will be approximately the same as for a crystal in a saturated solution. Further away from the crystal surface there is a depletion layer in which the concentration gradually changes from the saturation value ϕ_s to the value ϕ_0 far away in the solution (Figure 6).

As an example we present results for a protein with a molecular weight $M = 24400$ (this corresponds to $m = M/18\rho = 1000$ for $\rho = 1.36$ g.cm^{-3}), a coordination number in the crystal $z_c = 4$, and a solubility at 25 °C of $\phi_s = 0.005$. Figure 7 shows the calculated concentration profile of the interface layer at 25 °C for different values of the interaction parameter θ. The adsorbed amount of protein N_A at 25 °C as a function of θ is shown in Figure 8. We find that if the temperature T (in this case $T = 298$ K) is above the critical temperature T_0 for the metastable liquid−liquid phase separation (i.e., for $\theta/T < 1$) the concentration at the crystal surface ϕ_1 and the adsorbed amount of protein N_A are small. For temperatures near and below T_0 (i.e., $\theta/T \geq 1$) both N_A and ϕ_1 rapidly increase. The surface film is quite thin, with most of the excess protein being present in the layer between $x = 0$ and $x = 2a$ (Figure 7). Only when the temperature approaches to the triple point T_t (which in this case is at $\theta = \theta_t = 466$ K) does the width of the surface film increase strongly.[11,27]

In Figure 9 we show the calculated surface energy σ at 25 °C as a function of θ. The values of σ are compared with the surface energy σ_{00} which the crystal would have in the absence of a liquid surface film. We find that the presence of the surface film produces a lowering $\Delta\sigma$ of the surface energy, as expected; $\Delta\sigma$ rapidly increases with increasing θ. We conclude that the presence of a metastable liquid−liquid two-phase region leads to a substantial reduction of the surface energy.

8. Application to Lysozyme

We applied the preceding considerations to calculate the degree of aggregation of lysozyme molecules in solutions, the surface energy of lysozyme crystals, and the adsorbed amount of lysozyme present in the thin liquid film on the surface of

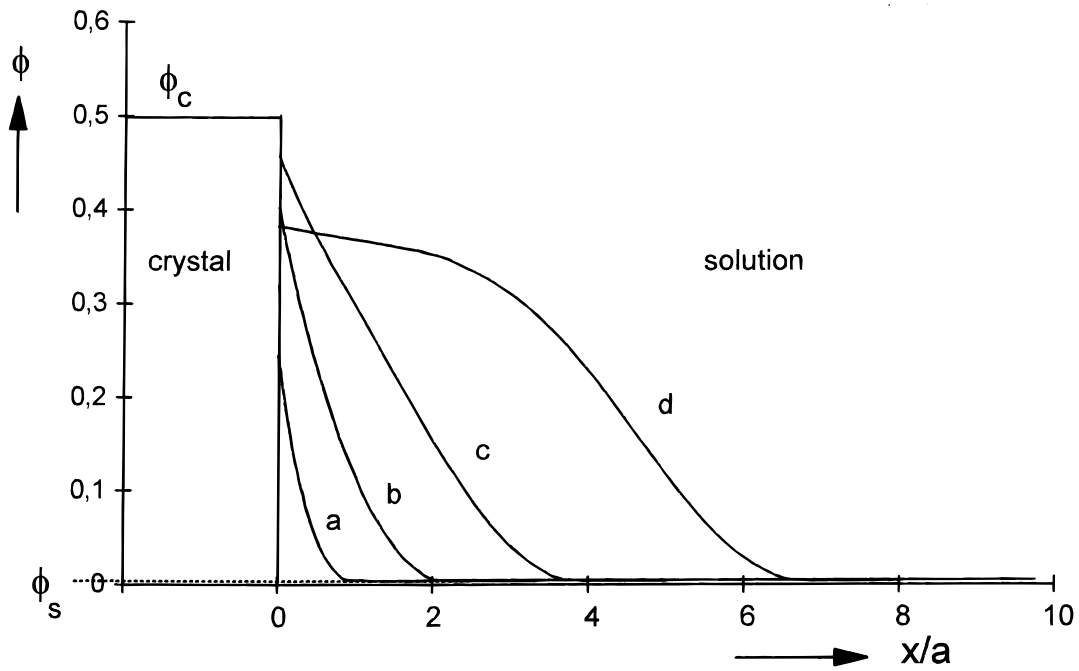

Figure 7. Concentration profile of the interface between a protein crystal and the saturated solution at 298 K for different values of the interaction parameter θ. The curves a, b, c, d are for θ values of 149, 298, 426, and 465 K, respectively. The data are for a protein with $M = 24400$, $z_c = 4$, and $\phi_s = 0.005$.

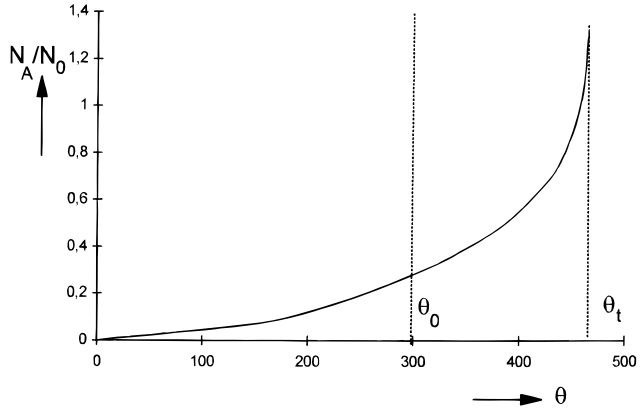

Figure 8. The number N_A of adsorbed protein molecules per cm^2 at 298 K (in units $N_0 = 1/(4a^2)$) as a function of the interaction parameter θ. For a value $\theta = \theta_0 = 298$ K the critical temperature for liquid−liquid phase separation is $T_0 = 298$ K (eq 5). For $\theta = \theta_t = 466$ K the triple point is $T_t = 298$ K. The data are for a protein with $M = 24400$, $z_c = 4$, and $\phi_s = 0.005$.

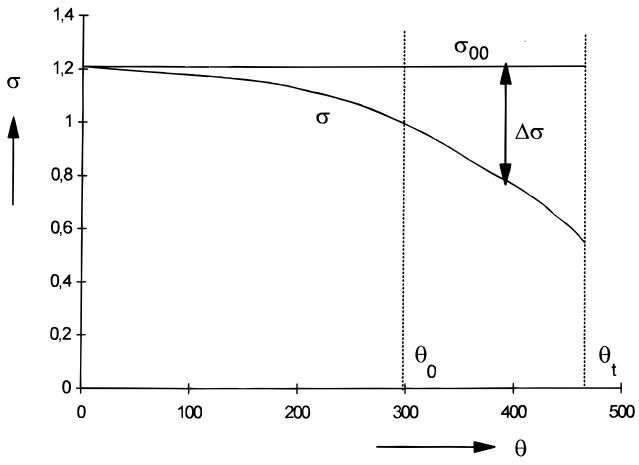

Figure 9. Surface energy σ (in units kT/a^2) of a protein crystal at 298 K as a function of the interaction parameter θ. The surface energy for a crystal without a surface film is σ_{00}. The surface film causes a lowering of the surface energy by $\Delta\sigma$. For a value $\theta = \theta_0 = 298$ K the critical temperature for liquid−liquid phase separation is $T_0 = 298$ K. For $\theta = \theta_t = 466$ K the triple point is $T_t = 298$ K. The data are for a protein with $M = 24400$, $z_c = 4$, and $\phi_s = 0.005$.

the crystal. For the calculations we used experimental data for the solubility ϕ_s[45] and the second virial coefficient B[46] of aqueous lysozyme solutions at 25 °C with pH = 4.2, containing 0.1 M HAc/NaAc and various concentrations of NaCl. For lysozyme $M = 14000$, $a = 1.6$ nm, and $z_l = 4$.[12]

Table 1 gives calculated values of the surface energy σ of lysozyme crystals and the number of adsorbed lysozyme molecules per cm^2 N_A (in units $N_0 = 1/(4a^2)$) . The surface energy of the crystal in equilibrium with the saturated solution is compared with the value σ_{00} of the surface energy of a crystal without a surface film;[47] the effect of the surface film is $\Delta\sigma = \sigma - \sigma_{00}$. We see that the surface film causes a substantial reduction of the surface energy, especially at large values of θ. The adsorbed amount of lysozyme increases strongly at large values of θ.

The average coordination number of protein molecules in an aqueous solution z_l is proportional to the concentration ϕ. Values of the ratio z_l/ϕ, calculated with eq 7, are given in Table 2. We find that the degree of aggregation, as characterized by z_l, strongly increases with increasing values of θ. Above the critical temperature for metastable liquid−liquid phase separation T_0 (i.e., for $\theta/T < 1$) z_l is smaller than 1 even for rather concentrated solutions, indicating that most lysozyme molecules are present as monomers ($z_l = 0$) or dimers ($z_l = 1$). Below T_0 (i.e., for $\theta/T > 1$) z_l has for concentrated solutions ($\phi \sim 0.3$) values between 1 and 2; thus in these solutions most of the lysozyme molecules are present in small aggregates of about four molecules or in larger, extended, open structures.

Experiments with ultracentifugation,[48,49] light scattering,[50] neutron scattering,[51−55] and dialysis[56] give evidence for the presence of small aggregates of lysozyme molecules in aqueous solutions. There are indications that small aggregates of about four lysozyme molecules act as precursors for the nucleation

TABLE 1: Surface Energy σ, Reduction $\Delta\sigma$ of the Surface Energy Due to the Presence of a Surface Film and Protein Molecules N_A Adsorbed at the Crystal Surface[a]

% NaCl	B (10^{-4} mol ml g^2)	ϕ_s	θ	N_A/N_0	σ_{00} (erg/cm^2)	σ (erg/cm^2)	$\Delta\sigma$ (erg/cm^2)
2	+0.1	0.041	107	0.23	0.80	0.72	−0.08
2.5	−1.6	0.018	198	0.52	0.97	0.80	−0.17
3	−3.2	0.011	284	0.85	1.05	0.78	−0.27
4	−4.4	0.0053	348	1.01	1.15	0.85	−0.30
5	−5.3	0.0028	396	1.06	1.21	0.93	−0.28
7	−7.4	0.0015	508	1.77	1.29	0.86	−0.43

[a] The data are for lysozyme solutions at 25 °C in 0.1 M Na−acetate buffer at pH 4.2 and with various concentrations of NaCl. Experimental data for ϕ_s and B are from refs 45 and 46, respectively. N_A is the number of adsorbed protein molecules per unit surface area, and $N_0 = 1/(4a^2)$.

TABLE 2: Aggregation of Lysozyme Molecules in Aqueous Solutions[a]

% NaCl	B (10^{-4} mol ml g^2)	ϕ_s	θ	$-g_l$ (10^{-21} J)	$-g_c$ (10^{-21} J)	z_l/ϕ
2	+0.1	0.041	107	7.8	39	1.6
2.5	−1.6	0.018	198	14.5	43	2.7
3	−3.2	0.011	284	21	45	3.7
4	−4.4	0.0053	348	26	48	4.3
5	−5.3	0.0028	396	29	50	4.6
7	−7.4	0.0015	508	37	53	5.6

[a] The degree of aggregation of the molecules in the solution is characterized by the average coordination number z_l; the concentration of lysozyme in the solution is ϕ. The data are for aqueous solutions at 25 °C in 0.1 M Na−acetate buffer and with various concentrations of NaCl. Experimental data for ϕ_s and B are from refs 45 and 46, respectively.

process. Kinetic studies[57−59] show that the rate of nucleation of lysozyme is proportional to the fourth power of the lysozyme concentration, indicating that the rate determining first step of the nucleation process is the forming of lysozyme tetramers. Electron microscopy studies[55] revealed the presence of linear chains of four lysozyme molecules in the initial phase of the nucleation process; in a later stage these tetramers coalesce to form spherical clusters ("rice balls"). These spherical clusters correspond presumably to the liquid droplets with a high protein concentration, proposed as an intermediate in the two-step nucleation mechanism.

Experiments with light scattering during nucleation and growth of lysozyme crystals[60−64] show aggregates with a fractal dimension smaller than three and with a size at the beginning of the nucleation process of $R_g = 3-6$ nm; at a later time larger fractal aggregates are observed. The radius of a lysozyme molecule being 1.6 nm, these R_g values indicate that the formation of small aggregates of 3−5 molecules is the first step in the nucleation process. The larger fractal aggregates would then correspond to the liquid droplets of the two-step nucleation mechanism.

9. Discussion of Nucleation and Crystal Growth

In this section we discuss the relation between the growth of protein crystals from an aqueous solution and the properties of the interface between the crystal and the solution.

We first discuss the case in which there is no region of metastable liquid−liquid phase separation close to the temperature of crystallization (i.e., for $T \gg T_0$). In this case the nucleation is expected to proceed by a one-step process, involving the formation of small crystalline nuclei in a dilute but supersaturated solution, as described by classical nucleation theory. The interface between the crystal and the solution in this case is quite sharp. The growth of the crystal involves the incorporation in the crystal of molecules which diffuse from the solution to the surface of the crystal. However, because of the large anisotropy of the interaction between the protein molecules, the probability that a protein molecule reaches the surface with the proper orientation for binding at the crystal is small. Thus, many of the molecules reaching the surface will diffuse back into the solution; the sticking probability is small. Moreover, those molecules which do stick to the surface must diffuse along the surface to the growth steps, and the crystal growth rate is strongly reduced.

The presence of a metastable liquid−liquid phase separation in the phase diagram has a profound influence on several aspects of the nucleation and crystal growth processes. Near and below the temperature for metastable liquid−liquid phase separation ($T \approx T_0$ and $T < T_0$) nucleation proceeds by a two-step mechanism. The first step is the formation of small liquid droplets with a high protein concentration. It is expected that, as a consequence of the high protein concentration, a large fraction of the molecules in these droplets are present in the form of molecular aggregates. For lysozyme there is evidence that the formation of these aggregates is the rate determining step of the nucleation process. After the formation of small liquid droplets with a high protein concentration, crystalline nuclei can form inside the droplets. These crystals will grow, but (as was shown in previous sections) for $T \approx T_0$ or $T < T_0$ they are permanently covered with a thin liquid film with a high protein concentration. This film lowers the surface energy of the crystal. Molecules, diffusing from the dilute solution to the crystal are easily incorporated in the liquid surface film. For this process there are no restrictions with regard to the orientation of the molecule, so that the sticking probability will be large. In the liquid surface film, the molecules or aggregates are quite mobile, and have ample time to find the proper orientation for incorporation in the crystal. Thus, the effects of the reduced sticking probability, expected for $T > T_0$ as a result of the anisotropy of the interactions between the protein molecules, will not be present for $T \approx T_0$ and $T < T_0$.

Because of the permanent presence of a thin liquid film with a high protein concentration on the surface, molecules are continuously found near the steps on the crystal surface and can easily attach in the proper orientation. Diffusion along the surface is not required. In addition, there will be an exchange of molecules between the liquid film and the surface layers of the crystal; this process could lead to the removal of crystalline defects in the surface layers of the crystal and reduce the incorporation of defects in the growing crystal. Thus, the presence of the liquid film possibly contributes not only to the growth speed but also to the quality of the growing crystal.

A nucleation mechanism in several steps, with first being the formation of small aggregates, followed by the coalescence of aggregates to form larger disordered regions with a high concentration (liquid droplets, "rice balls", etc.), has been discussed for several types of systems.[59−70]

10. Conclusions

The concentration profile of the interface between a protein crystal and an aqueous solution is determined by the contribution of concentration gradient terms to the Gibbs free energy of the solution. We derived a relation between the parameter for this contribution and the interaction potential between protein molecules. With this result it is possible to calculate quantitatively the concentration profile and the surface energy.

The calculations show that the presence of a metastable liquid−liquid phase separation region in the phase diagram has a profound effect on the interface profile. For temperatures near and below the critical temperature T_0 for the liquid−liquid phase separation protein crystals are covered by a thin liquid film with a high protein concentration, which lowers the surface energy of the crystal. The presence of the liquid film has a strong influence on the growth of crystals. In the absence of a surface film the sticking probability of protein molecules at the surface is small, due the high anisotropy of protein−protein interactions. However, in the presence of a liquid surface film with a high protein concentration, molecules are always available at the growth steps and diffusion along the surface is not required. A molecule in the film has ample time to find the proper orientation for bonding at the crystal. Thus, the liquid surface film present at temperatures near and below T_0 will enhance the sticking probability.

Experimental data of the solubility and the second virial coefficient of lysozyme was used to calculate the surface energy of lysozyme crystals. This energy is appreciably reduced if a liquid film with a high concentration of lysozyme molecules is present on the surface of the crystals. This liquid film can be considered as an adsorption of molecules at the surface of the protein crystal. It is expected that a metastable liquid−liquid immiscibility region will also enhance the adsorption of protein molecules on other types of surfaces, such as glass walls or the air−water interface.

Finally, we remark that the theoretical considerations in this paper contain many approximations. For example, the phase diagram is calculated with a mean-field type theory, which cannot describe quantitatively the shape of the liquid−liquid immiscibilty region, in particular near the critical point T_0. The calculations for the interface also involve approximations, such as the use of a constant value of the parameter κ for the complete concentration range up to ϕ_c. Therefore, the results are not accurate in a quantitative sense, but it is expected that they describe in a satisfactory way the characteristic features of the phase diagram and the interface between a crystal and the solution, and can serve as a guide in the interpretation of data on crystal growth.

Acknowledgment. This work was supported by the Commission of the European Community under contract B104-CT98-0086.

References and Notes

(1) Darcy, P. A.; Wiencek, J. M. *J. Cryst. Growth* **1999**, *196*, 243.
(2) Broide, M. L.; Tominc, T. M.; Saxowsky, M. D. *Phys. Rev.* **1991**, *E53*, 632.
(3) Thomson, J. A.; Schurtenberger, P.; Thurston, G. M.; Benedek, G. B. *Proc. Natl. Acad. Sci. U.S.A.* **1987**, *84*, 7079.
(4) Schurtenberger, P.; Chamberlin, R. A.; Thurston, G. M.; Thomson, J. A.; Benedek, G. B. *Phys. Rev. Lett.* **1989**, *63*, 2064.
(5) Broide, M. L.; Berland, C. R.; Pande, J.; Ogun, O.; Benedek, G. B. *Proc. Natl. Acad. Sci. U.S.A.* **1991**, *88*, 5660.
(6) Berland, C. R.; Thurston, G. M.; Kondo, M.; Broide, M. L.; Pande, J.; Ogun, O.; Benedek, G. B. *Proc. Natl. Acad. Sci. U.S.A.* **1992**, *89*, 1214.
(7) Fine, B. M.; Pande, J.; Lomakin, A.; Ogun, O.; Benedek, G. B. *Phys. Rev. Lett.* **1995**, *74*, 1981.
(8) Liu, C.; Lomakin, A.; Thurston, G. M.; Hayden, D.; Pande, A.; Pande, J.; Ogun, O.; Asherie, N.; Benedek, G. B. *J. Phys. Chem.* **1995**, *99*, 454.
(9) Asherie, N.; Lomakin, A.; Benedek, G. B. *Phys. Rev. Lett.* **1996**, *76*, 4832.
(10) Lekkerkerker, H. N. W. *Physica* **1997**, *A244*, 227.
(11) Haas, C.; Drenth, J. *J. Phys. Chem. B* **1998**, *102*, 4225.
(12) Haas, C.; Drenth, J.; Wilson, W. W. *J. Phys. Chem. B* **1999**, *103*, 2808.
(13) Neal, B. L.; Asthagiri, D.; Velev, O. D.; Kaler, E. W.; Lenhoff, A. M. *J. Cryst. Growth* **1999**, *196*, 377.
(14) Rosenbaum, D.; Zamora, P. C.; Zukoski, C. F. *Phys. Rev. Lett.* **1996**, *76*, 150.
(15) Lomakin, A.; Asherie, N.; Benedek, G. B. *J. Chem. Phys.* **1996**, *104*, 1646.
(16) Malfois, M.; Bonneté, F.; Belloni, L.; Tardieu, A. *J. Chem. Phys.* **1996**, *105*, 3290.
(17) George, A.; Wilson, W. W. *Acta Crystallogr.* **1994**, *D50*, 361.
(18) George, A.; Chiang, Y.; Guo, B.; Arabshaki, A.; Cai, Z.; Wilson, W. W. *Methods Enzymol.* **1997**, *276*, 100.
(19) ten Wolde, P. R.; Frenkel, D. J. *Science* **1997**, *277*, 1975.
(20) Giegé, B.; Drenth, J.; Ducruix, A.; McPherson, A.; Saenger, W. *Prog. Cryst. Growth Charact.* **1995**, *30*, 251.
(21) Drenth, J.; Haas, C. *Acta Crystallogr.* **1998**, *D54*, 867.
(22) Talanquer, V.; Oxtoby, D. W. *J. Chem. Phys.* **1998**, *109*, 223.
(23) Evans, R. M. L.; Poon, W. C. K. *Phys. Rev.* **1997**, *E56*, 5748.
(24) Evans, R. M. L.; Cates, M. E. *Phys. Rev.* **1997**, *E56*, 5738.
(25) Evans, R. M. L. *Europhys. Lett.* **1997**, *38*, 595.
(26) Chernov, A. A. *Modern Crystallography*, vol. III, Springer Series in Solid State Sciences; Springer: Berlin, 1984.
(27) Haas, C.; Drenth, J. *J. Cryst. Growth* **1999**, *196*, 388.
(28) Ilet, S. M.; Orrock, A.; Poon, W. C. K.; Pusley, P. N. *Phys. Rev.* **1998**, *E51*, 1344.
(29) Tejero, C. F.; Daanoun, A.; Lekkerkerker, H. N. W.; Baus, M. *Phys. Rev. Lett.* **1994**, *73*, 752.
(30) Tejero, C. F.; Daanoun, A.; Lekkerkerker, H. N. M.; Baus, M. *Phys. Rev.* **1995**, *E51*, 558.
(31) Hagen, M. H. J.; Frenkel, D. J. *J. Chem. Phys.* **1994**, *101*, 4093.
(32) Hagen, M. H. J.; Meijer, E. J.; Mooij, C. A. M.; Frenkel, D. J.; Lekkerkerker, H. N. M. *Nature* **1993**, *365*, 425.
(33) Poon, W. C. K. *Phys. Rev.* **1997**, *E55*, 3762.
(34) Taratuta, V. G.; Holockbach, A.; Thurstein, G. M.; Blankschtein, D. B.; Benedek, G. B. *J. Phys. Chem.* **1990**, *94*, 2140.
(35) Muschol, M.; Rosenberger, F. *J. Chem. Phys.* **1997**, *107*, 1953.
(36) Lomakin, A.; Asherie, N.; Benedek, G. B. *Proc. Natl. Acad. Sci. U.S.A.* **1999**, *96*, 9465.
(37) Sear, R. P. *J. Chem. Phys.* **1999**, *111*, 4800.
(38) Overbeek, J. Th. G. *Faraday Discuss.* **1978**, *65*, 7.
(39) Carnahan, N. F.; Starling, K. F. *J. Chem. Phys.* **1969**, *51*, 635.
(40) Cahn, J. W.; Hilliard, J. E. *J. Chem. Phys.* **1958**, *28*, 258.
(41) Cahn, J. W. *J. Chem. Phys.* **1977**, *66*, 3667.
(42) de Gennes, P. G. *Rev. Mod. Phys.* **1985**, *57*, 827.
(43) Landau, L. D.; Lifshitz, E. M. *Statistical Physics;* Pergamon: Oxford, 1980; vol. 5, part I.
(44) Li, H.; Perozzo, M. A.; Konnert, J. H.; Nadarajah, A.; Pusey, M. L. *Acta Crystallogr.* **1999**, *D55*, 1023.
(45) Cacioppo, E.; Pusey, M. *J. Cryst. Growth* **1991**, *114*, 286.
(46) Guo, B.; Kao, S.; McDonald, H.; Wilson, W. W.; Asanov, A.; Combs, L. L. *J. Cryst. Growth* **1999**, *196*, 424.
(47) Haas, C.; Drenth, J. *J. Cryst. Growth* **1995**, *58*, 126.
(48) Sophianopoulos, A. J.; Holde, K. E. *J. Biol. Chem.* **1964**, *239*, 2516.
(49) Behlke, J.; Knespel, A. *J. Cryst. Growth* **1996**, *158*, 388.
(50) Pusey, M. L. *J. Cryst. Growth* **1991**, *110*, 60.
(51) Boué, F.; Lefaucheux, F.; Robert, M. C.; Rosenman, I. *J. Cryst. Growth* **1998**, *133*, 246.
(52) Minezaki, Y.; Nimura, N.; Ataka, M. *Biophys. Chem.* **1996**, *58*, 355.
(53) Niimura, N.; Minezaki, Y.; Ataka, M.; Katsura, T. *J. Cryst. Growth*, **1995**, *154*, 136.
(54) Niimura, N.; Minezaki, Y.; Tanaka, T.; Fujiwara, S.; Ataka, M. *J. Cryst. Growth* **1999**, *200*, 265.
(55) Nichinomae, M.; Mochizuki, M.; Ataka, M. *J. Cryst. Growth* **1999**, *197*, 257.
(56) Wilson, L. J.; Adcock-Downey, L.; Pusey, M. L. *Biophys. J.* **1996**, *71*, 2123.
(57) Ataka, M.; Asai, M. *Biophys. J.* **1990**, *58*, 807.
(58) Eigersma, A. V.; Ataka, M.; Katsura, J. *J. Cryst. Growth* **1992**, *122*, 31.

(59) Nadarajah, A.; Pusey, M. L. *Acta Crystallogr.* **1998,** *D53*, 524.
(60) Georgalis, Y.; Umbach, P.; Zielenkiewicz, A.; Utzig, E.; Zielenkiewicz, W.; Zielenkiewicz, P.; Saenger, W. *J. Am. Chem. Soc.* **1997**, *119*, 11959.
(61) Georgalis, Y.; Umbach, P.; Raptis, J.; Saenger, W. *Acta Crystallogr.* **1997**, *D53*, 691.
(62) Georgalis, Y.; Umbach, P.; Soumpasis, D. M.; Saenger, W. *J. Am. Chem. Soc.* **1998**, *120*, 5539.
(63) Umbach, P.; Georgalis, Y.; Saenger, W. *J. Am. Chem. Soc.* **1998**, *120*, 2382.
(64) Georgalis, Y.; Umbach, P.; Saenger, W.; Ihmels, B.; Soumpasis, D. M. *J. Am. Chem. Soc.* **1999**, *121*, 1627.
(65) Kuznetsev, Yu. G.; Malkin, A.; McPherson, A. *J. Cryst. Growth* **1999**, *196*, 489.
(66) Vliegenthart, G. A.; van Blaaderen, A.; Lekkerkerker, H. N. W. *Faraday Discuss.* **1999**, *112.*
(67) de Moor, P.-P. E. A.; Beelen, T. P. M.; Komanschek, B. U.; Beck, L. W.; Wagner, P.; Cavis, M. E.; van Santen, R. A. *Chem. Eur. J.* **1999**, *5*, 2083.
(68) Dokter, W. H.; van Garderen, H. F.; Beelen, T. P. M.; van Santen, R. A.; Bras, W. *Angew. Chem., Int. Ed. Engl.* **1995**, *34*, 73.
(69) Hobbie, E. K. *Phys. Rev. Lett.* **1998**, *81*, 3996.
(70) Soga, K. G.; Melrose, J. R.; Ball, R. C. *J. Chem. Phys.* **1999**, *110*, 2280.